REFERÊNCIA

NASCIMENTO, Ana P.; LINARES, José J. Performance of a direct glycerol fuel cell using KOH doped polybenzimidazole as electrolyte. **Journal of the Brazilian Chemical Society**, São Paulo, v. 25, n. 3, p. 509-516, mar. 2014. Disponível em: http://www.scielo.br/scielo.php?script=sci_arttext&pid=S0103-50532014000300014&lng=en&nrm=iso. Acesso em: 13 dez. 2019.

http://dx.doi.org/10.5935/0103-5053.20140018

J. Braz. Chem. Soc., Vol. 25, No. 3, 509-516, 2014.
Printed in Brazil - ©2014 Sociedade Brasileira de Química
0103 - 5053 $6.00+0.00

Article

Performance of a Direct Glycerol Fuel Cell using KOH Doped Polybenzimidazole as Electrolyte

Ana P. Nascimento and José J. Linares*

Instituto de Química, Universidade de Brasília, Campus Darcy Ribeiro, CP 4478, 70910-900 Brasília-DF, Brazil

Este trabalho mostra os resultados correspondentes ao estudo da influência das variáveis de operação (temperatura, concentração de glicerol, de KOH e vazão de alimentação) de uma célula a combustível de glicerol direto usando o polibenzimidazol (PBI) impregnado com KOH como eletrólito e Pt/C como catalisador. A temperatura mostra um efeito favorável até o valor limite de 75 °C, causado por melhoras na condutividade e na cinética. A concentração ótima do combustível que alimenta a célula é de 1 mol L^{-1} em KOH 4 mol L^{-1}, fornecendo suficiente quantidade de combustível e de eletrólito sem cruzamento massivo ao cátodo nem limitações de transferência de matéria. A vazão de alimentação melhora o desempenho até um valor limite de 2 mL min^{-1}, suficiente para garantir o acesso do glicerol e a saída dos produtos. Finalmente, o uso de catalisadores binários (PtRu/C e Pt_3Sn/C) resulta benéfico para incrementar o desempenho do sistema.

This paper studies the influence of the operating variables (glycerol concentration, temperature and feed rate) for a direct glycerol fuel cell fed with glycerol using polybenzimidazole (PBI) impregnated with KOH as electrolyte and Pt/C as catalyst. Temperature displays a beneficial effect up to 75 °C due to the enhanced conductivity and kinetics of the electrochemical reactions. The optimum cell feed corresponds to 1 mol L^{-1} glycerol and 4 mol L^{-1} KOH, supplying sufficient quantities of fuel and electrolyte without massive crossover nor mass transfer limitations. The feed rate increases the performance up to a limit of 2 mL min^{-1}, high enough to guarantee the access of the glycerol and the exit of the products. Finally, the use of binary catalysts (PtRu/C and Pt_3Sn/C) is beneficial for increasing the cell performance.

Introduction

The rapid growth of the biodiesel industry in the last 10 years demands solutions to the glycerol byproduct produced by transesterification of a triglyceride and an alcohol (1 kg *per* 10 kg of biodiesel).[1] Glycerol has traditionally been absorbed by the pharmaceutical, cosmetic, agro and food industries.[2] However, the current production rate already surpasses their capacities. Brazil is the third largest global producer of biodiesel (46,058 barrels per day in 2011), with exponential growth since 2005.[3] Moreover, the central-west region alone supported half this production.[4]

One alternative proposed to valorize the glycerol molecule is oxidation, giving rise to more oxygenated compounds with greater added value: tartronic acid, mesoxalic acid, β-hydroxypiruvic acid, dihydroxyacetone, and glycolic acid, among others.[5] The classical processes for obtaining these products involve the use of environmentally unfriendly oxidants such as $KMnO_4$, HNO_3 or H_2CrO_4. Biological fermentation is another alternative that overcomes the environmental issues. However, the operational conditions need to be strictly controlled and the kinetics of these processes is rather sluggish.[6,7] Heterogeneous catalysis is another alternative, showing interesting results with materials such as PtPd, PtAu, PtBi, PtNi, AuPd, PtPdBi.[8-17] In this case, glycerol is oxidized in the presence of oxygen, with significant activity in alkaline media.

These results opened the possibility for using glycerol as a direct fuel in a direct glycerol fuel cell (DGFC), with the emphasis on operation in an alkaline environment. Matsuoka *et al.*[18] implemented an alkaline DGFC for the first time in 2005 using a Tokuyama anion exchange membrane. Subsequent fuel cell studies to date have focused on the use of anionic exchange membranes, such as Tokuyama (A201 and A901) and ADP-Morgane.[14,19-23] One possible alternative to these membranes is polybenzimidazole (PBI) impregnated with KOH. PBI is an amphoteric polymer that can interact with acids and alkalis. In the latter case, the existence of amine (NH) groups in its structure allows

*e-mail: joselinares@unb.br

interaction with inorganic hydroxides such as KOH. In this regard, interesting results have been obtained with methanol and ethanol.[24-28]

On the other hand, the development of catalysts for glycerol oxidation is also an active field. Noble metals (Pt, Au and Pd) have emerged as the most effective materials for glycerol electroxidation as shown by numerous studies,[23,28-34] with the addition of other secondary metals that promote electrocatalytic activity and/or modify selectivity towards a certain oxidation product.[35,36] Nevertheless, up to now, the most efficient materials for glycerol oxidation are Pt and Pt-based ones.

In this context, this study aims at developing an alkaline-based DGFC using PBI impregnated with KOH as an electrolyte, for the purpose of studying the influence of the operating conditions on cell performance: the temperature, glycerol concentration, KOH concentration in the fuel and fuel feed rate. Once the operating conditions were optimized, commercial bimetallic PtRu/C and Pt_3Sn/C were used as anode catalysts in order to obtain a preliminary evaluation of the impact of adding a second less noble metal.

Experimental

The fuel cell electrodes were prepared as follows: a thick ink consisting of Pt/C (20% Pt/C, BASF Fuel Cells, formerly ETEK-Inc.), Nafion® emulsion (10% wt. with respect to the carbon loading in the catalytic layer), and isopropanol as solvent was prepared, ultrasonicated for 5 min and allowed to dry. Next, a few drops of isopropanol were added until a new slurry was formed that was applied with the aid of a paintbrush onto the gas diffusion layer (GDL). This was composed of carbon powder (Vulcan XC-72R) and 15 wt.% PTFE (TE-3893, Dupont), which was applied homogenously over a carbon cloth (PWB-3, Stackpole) by vacuum filtration. The GDL was kindly donated by the Electrochemistry Group of the Institute of Chemistry of São Carlos (University of São Paulo). After applying the catalytic layer, the electrodes were cured at 80 °C for 1 h in order to ensure evaporation of the solvent. The final Pt loading in the anode was 2 mg cm^{-2}, whereas the corresponding loading in the cathode was 1 mg cm^{-2}. The active area of the electrodes was 0.785 cm^2. Binary catalysts (20% PtRu/C, atomic ratio 1:1 , BASF Fuel Cells, formerly ETK-Inc., and 20% Pt_3Sn/C, atomic ratio 3:1, from the same supplier) were prepared following the same protocol, with a final metal loading of 2 mg cm^{-2}.

The membrane electrode assembly (MEA) was prepared by sandwiching the electrodes between 2 pieces of polybenzimidazole (PBI, Danish Power System, Denmark) membrane. In order to provide anionic conductivity, the membrane was immersed in 6 mol L^{-1} KOH for at least one week. The adhesion between the membrane and the electrodes took place within the fuel cell rig itself, without performing any hot pressing procedure.

Electrochemical measurements were carried out with the aid of a potentiostat/galvanostat AUTOLAB PGSTAT 302 (Metrohm Autolab B.V., The Netherlands) in potentiostatic mode, from open circuit voltage (OCV) to lower cell voltages. Evaluation of the uncompensated resistance of the system was carried out with the frequency response analyzer (FRA) module of the potentiostat/galvanostat. The dc bias potential was fixed at 0.6 V, onto which a sinusoidal wave with a frequency ranging from 10 kHz to 100 Hz and an amplitude of 5 mV rms was applied.

The cell hardware consisted of two monopolar plates made of graphite with 2 parallel channels in a serpentine geometry. The end current collector plates were made of aluminum, into which heating rods were inserted in order to heat up the system. A hole for inserting a K-thermocouple connected to a temperature controller (N1020, Novus Instrumentation) was drilled into the graphite plate. For impulsion of the glycerol solution, a diaphragm metering pump (Prominent) was used. The oxygen flow was controlled with the aid of a flow meter RMS-11 (Digiflow), fixing a value of 20 mL min^{-1}. A schematic drawing of the experimental setup is displayed in Figure 1.

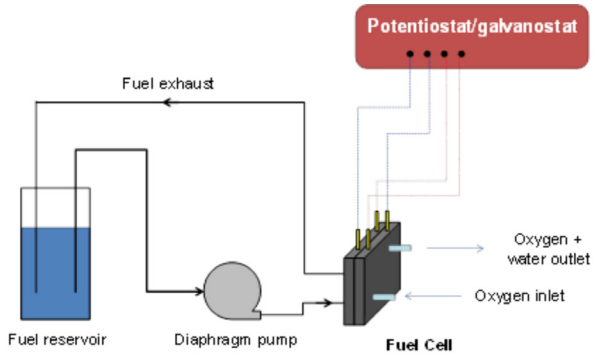

Figure 1. Experimental setup used in this study.

Results and Discussion

Influence of temperature

Figure 2a displays the polarization and power curves of the DGFC at five different temperatures (30, 45, 60, 75 and 90 °C). As expected, an increase in the cell temperature led to an enhancement in the cell performance up to 75 °C, with a maximum power density of 18 mW cm^{-2}. This can be explained in terms of the improved kinetics of the glycerol electroxidation and oxygen reduction reactions. Special attention should be paid to the first process. Glycerol is

a complex molecule with one OH^- group on each carbon atom of the molecule. Its oxidation can give rise to a large number of adsorbed species that can severely poison the catalyst surface.[37] An increase in the temperature is expected to alleviate this. Concurrently, the uncompensated resistance in the system, whose main contribution is the ohmic resistance of the membrane, is expected to decrease. Figure 2b shows the increase in membrane conductivity (see equation 1 for the membrane conductivity (σ) calculation, where R is the ohmic resistance from the high frequency intercept of the Nyquist plot with the real axis, δ is the membrane thickness and A is the cross-sectional area) up to 75 °C. However, when the temperature achieved a value of 90 °C, there was a decrease in performance. In principle, the conductivity of any KOH solution increases with the temperature, due to the greater mobility of the ions in the solution.[38] However, at a certain temperature, the conductivity has a maximum at an intermediate KOH concentration, and decreases for more highly concentrated solutions due to the increase in viscosity. Also, the higher the temperature, the higher the water vapor partial pressure becomes,[39] accelerating the vaporization process of the hypothetical solution despite the increase in the water boiling point by the presence of KOH.

$$\sigma = \frac{1}{R} \cdot \frac{\delta}{A} \quad (1)$$

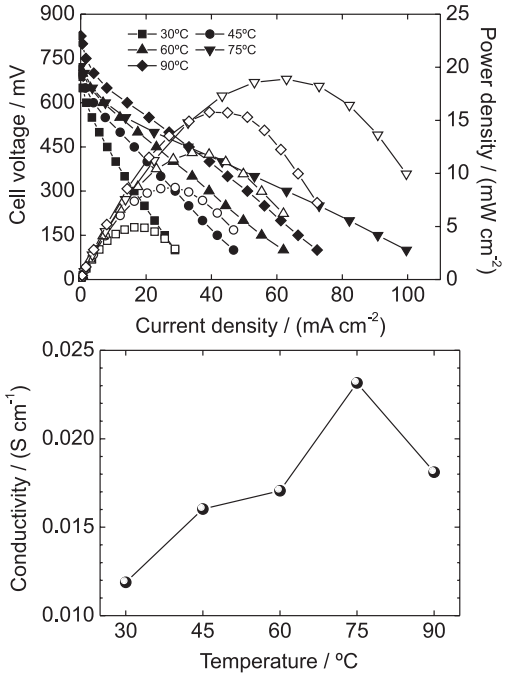

Figure 2. (a) fuel cell performance for different temperatures in the alkaline DGFC (glycerol concentration: 1 mol L^{-1}; KOH concentration: 4 mol L^{-1}; oxygen as comburent with a flow rate of 20 mL min^{-1}; anode flow rate of 1 mL min^{-1}) and (b) membrane conductivity at different temperatures.

The conductivity reported in Figure 2a is primarily determined by the ionic mobility in the MEA, including the electrodes and the membrane. In principle, the supply of a liquid fuel in the anode must guarantee the mobility of the OH^- anions. In the case of the membrane, a similar scenario could be expected, since this is expected to become equilibrated with the anode solution. However, the cathode environment is more complex. Oxygen is fed without humidification, and the cathodic reaction requires water to form the OH^- that will be transported to the anode. The only source of water is the flow permeating across the membrane. Furthermore, the alkaline environment at the cathode is maintained by the impregnation of the electrolyte with KOH, without a constant supply of the OH^- species from the anode. At high temperature, the water balance necessary to guarantee an efficient oxygen reduction reaction becomes more problematic. Moreover, the higher water vapor partial pressure in combination with a quite anhydrous environment (dry oxygen gas) may contribute to dehydration of the electrolyte with a consequent decrease in conductivity. This could explain the observed decrease in the cell performance. Nevertheless, new studies on the importance of cathode humidification are being carried out in order to confirm this. Therefore, operation at temperatures above 75 °C is not recommended for this KOH-impregnated PBI system without pre-humidification of the cathode stream.

Influence of glycerol concentration

Another important operating variable is the fuel concentration in the anode stream. This variable needs to be optimized since two antagonistic processes affect cell performance: access to sufficient fuel and fuel crossover. Fuel access to the catalytic sites must be guaranteed in order to have a satisfactory cell performance, especially at maximal current density where more glycerol is demanded. An increase in glycerol concentration intensifies the driving force for mass transfer processes. In contrast, a high glycerol concentration is unfavorable in terms of larger amounts of glycerol crossing to the cathode. This latter phenomenon depolarizes it, leading to reduced efficiency, OCV (mixed potential effect) and cell performance. Figure 3 shows the corresponding polarization curves for the different glycerol concentrations. The results are displayed for a temperature of 60 °C.

As can be seen, the maximum cell performance was achieved for a glycerol concentration of 1 mol L^{-1}. At a glycerol concentration of 0.5 mol L^{-1}, the cell performance at low current densities resembled that at 1 mol L^{-1}. However, above 35 mA cm^{-2} the cell performance dropped,

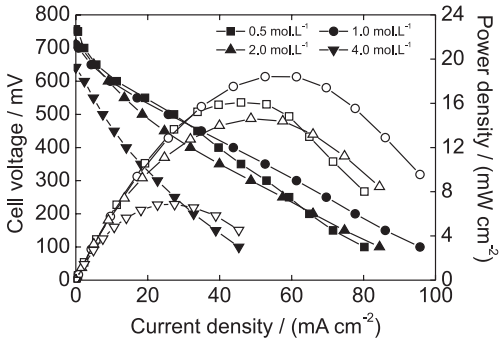

Figure 3. Fuel cell performance for different glycerol concentrations in the alkaline DGFC (temperature: 60 °C; KOH concentration: 4 mol L^{-1}; oxygen as comburent with a flow rate of 20 mL min^{-1}; anode flow rate of 1 mL min^{-1}).

most likely due to an insufficient amount of glycerol accessing the catalytic layer. A glycerol concentration of 2 mol L^{-1} also reduced cell performance compared to the reference value of 1 mol L^{-1}, and even more drastic results were evident at a glycerol concentration of 4 mol L^{-1}. In this latter case, the OCV was much lower, reflecting the deleterious effects of the fuel crossover. Moreover, glycerol possesses a dynamic viscosity of 81.3 cP at 60 °C, whereas in the case of water the corresponding value is 0.4688 cP. Hence, more concentrated glycerol solutions become more viscous. The greater viscosity could limit fuel transport to the catalytic layer. Also, the increase in the glycerol concentration could lead to a poisoning of the anode surface by virtue of the large amounts of this molecule competing with the hydroxyl radicals required for glycerol oxidation.[19,21] In the case of a fuel concentration of 2 mol L^{-1} fuel, these phenomena are also occurring, however to a lesser extent since the decrease in the performance is smaller. Finally, changes in the glycerol electroxidation mechanism depending on the glycerol concentration must also be taken into account, as Zhang *et al.*[20] showed. Higher glycerol concentrations favored the conversion of glycerol to less oxidized C_3-species, with faster turnover rates compared to lower concentrations. At lower concentrations, more oxidized products (tartronic acid and C_2 species) were produced. Currently, ongoing research is being carried out in order to better understand the oxidation mechanism under actual fuel cell conditions with the support of a liquid chromatograph.

Combined influence of glycerol concentration and temperature

Although previous sections show the results corresponding to one particular glycerol concentration and temperature, respectively, a more extensive study was also carried out. A combination of five temperatures and four glycerol concentrations was screened in its entirely, in order to study the combined effect of these parameters. For a simpler comparison, Figure 4 shows the maximum power density and OCV obtained for each condition.

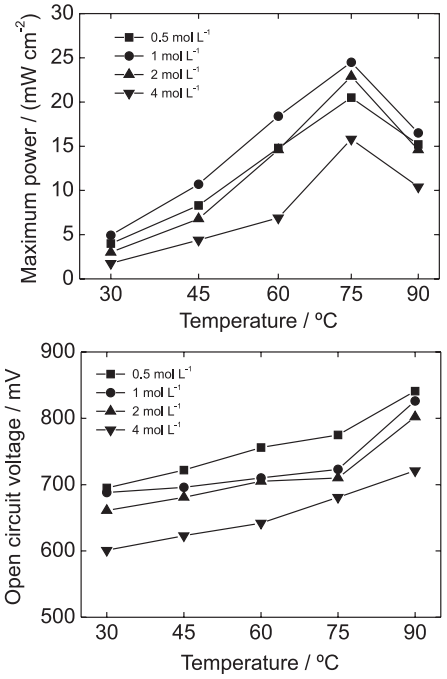

Figure 4. (a) maximum power density, and (b) open circuit voltage obtained in the alkaline DGFC at different temperatures and glycerol concentrations (KOH concentration: 4 mol L^{-1}; oxygen as comburent with a flow rate of 20 mL min^{-1}; anode flow rate of 1 mL min^{-1}).

As can be seen, an increase in the temperature always had a beneficial effect on cell performance, independent of the glycerol concentration, up to the limit value of 75 °C. At 90 °C, the ohmic resistance of the system rose upward unacceptably, leading to a decrease in cell performance. However, looking in more detail at the increase in maximum power, it can be seen that this is more pronounced at the highest glycerol concentrations, i.e., 2 mol L^{-1} and 4 mol L^{-1}. The maximum power density is normally achieved in the intermediate/high current density/voltage region of the polarization curve. In this, mass transfer processes exert a strong influence on cell performance, so that any increase in temperature is expected to decrease the viscosity and, consequently, enhance mass transfer processes within the electrode structure. Furthermore, the anode poisoning effect present at high glycerol concentrations (2 and 4 mol L^{-1}, as aforementioned) is expected to ameliorate the higher temperature. In fact, at 75 °C, the maximum power when operating with a 2 mol L^{-1} glycerol solution outperforms that with 0.5 mol L^{-1}. The open circuit voltage showed an increase with temperature. Although a higher glycerol crossover should be expected at higher temperatures, the

cathode seems to be more tolerant to the crossed over alcohol. Glycerol is more rapidly oxidized, releasing active sites for the oxygen reduction reaction. Furthermore, the operation of this latter reaction is promoted in alkaline fuel cells.[40]

Influence of KOH concentration in the feed

In alkaline exchange fuel cells, it is necessary to provide OH^- species from the feed solution in order to guarantee the alkaline environment in the anode, ensure an abundance of OH^- anions and stabilize the acidic oxidation products generated by the glycerol oxidation: glycolic, glyceric, mesoxalic, oxalic and formic acid and CO_2, which can reduce the pH locally. Figure 5 shows the influence of KOH concentration on cell performance. Furthermore, in order to assist in interpreting the results, Figure 5 also includes the value of the electrolyte conductivity of the KOH-impregnated membrane.

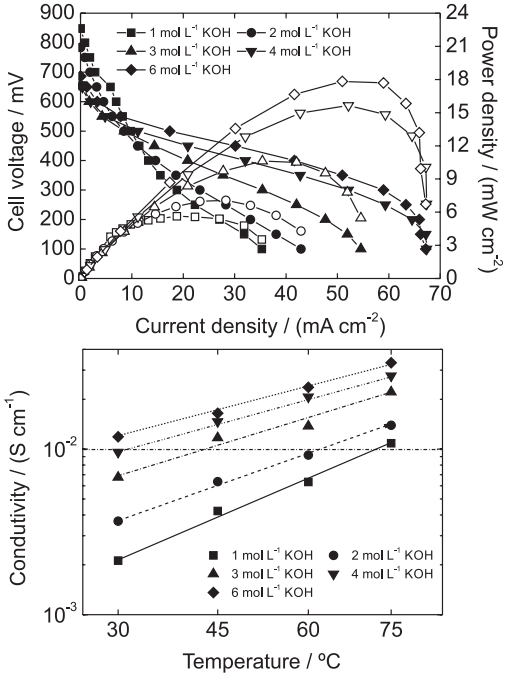

Figure 5. (a) fuel cell performance of the alkaline DGFC at different concentrations of KOH (glycerol concentration: 1 mol L^{-1}; temperature: 60 °C; oxygen as comburent with a flow rate of 20 mL min^{-1}; anode flow rate of 1 mL min^{-1}); and (b) membrane conductivity at different KOH concentrations and cell temperatures.

Some interesting tendencies can be observed in the polarization curves. At low current densities, the lower the KOH concentration, the better the performance, in spite of the reduced conductivity. Also, the OCV increases as the KOH concentration is lowered. In order to understand these results, it is necessary to assume that the membrane will always equilibrate with its environment, which is reasonable taking into account its operation using a liquid fuel. The lower the KOH, the lower the impregnation level of KOH becomes, which indeed reflects on the reduced conductivity. Along with KOH, some glycerol can also impregnate the membrane and reach the cathode. The lower the KOH concentration, the smaller the impregnation level which, in turn, will result in a smaller amount of glycerol crossing the membrane. However, at intermediate current densities, where the ohmic polarization governs performance, a high KOH concentration is beneficial due to the higher OH^- conductivity (see Figure 5b), especially at the highest temperature (higher OH^- mobility). Finally, at high current densities, mass transfer limitations noticeably impair cell performance at the highest concentrations (4 mol L^{-1} and 6 mol L^{-1}), reaching a maximum current density of ca. 70 mA cm^{-2} not achieved at the other lower KOH concentrations. At such high KOH concentrations, the viscosity of the solution also increases, impairing the convective and diffusive processes in the electrode and leading to the appearance of a limiting current density. A final issue that should be considered from a practical point of view is corrosion by the detrimental action of temperature and high KOH concentration. In fact, for this particular system, the use of 6 mol L^{-1} KOH leads to severe corrosion problems, especially in the aluminum end plates, with the formation of a non-conductive layer of potassium aluminate. This raises another important challenge that needs to be overcome: the development of alkaline resistant fuel cell plates for long-term operation. Hence, an adequate KOH concentration might be 4 mol L^{-1}. Nevertheless, it should be born in mind that a higher KOH concentration still enhances cell performance and that more advanced gas diffusion layers, especially designed for alkaline fuel cells, will reduce mass transfer limitations.

One final observation regarding the influence of the KOH concentration on cell performance is that, as in the case of the influence of glycerol concentration, the glycerol electroxidation mechanism is affected by this parameter. The balance of OH^- and glycerol (glycoxide) coverage is affected by the KOH concentration. A greater concentration of KOH will increase the OH^- coverage, and this species is necessary to oxidize the glycerol molecule. Also, higher pH favors the formation of the glycoxide anion, a more electroactive species, resulting in a deeper and more rapid oxidation of the glycerol molecule.[20] This undoubtedly affects the cell performance and explains the enhancement in cell performance observed with increasing glycerol concentrations within the range of low and intermediate current densities. Nevertheless, ongoing research is being done by this research group in order to better interpret this.

Influence of the feed rate

The feed rate is an important parameter directly related to mass transfer processes (see equation 2). Any change in the flow velocity is expected to influence the cell performance, especially at the highest current densities. Figure 6 shows the cell performance at different feed flow rates for a fuel solution of 1 mol L^{-1} glycerol 4 mol L^{-1} KOH.

As can be seen, there is an increase in cell performance with increasing feed rate in the intermediate-high current density region, where mass transfer processes become more influential on cell performance. The performance is enhanced up to a flow rate of 2 mL min^{-1} due to the improved mass transfer processes, but does not increase further with a flow rate of 4 mL min^{-1}. Hence, for this particular system, with a 0.785 cm^2 electrode and a Pt loading of 2 mg cm^{-2}, and using an anode feed solution with 1 mol L^{-1} glycerol and 4 mol L^{-1} KOH, the optimum anode flow rate is 2 mL min^{-1}.

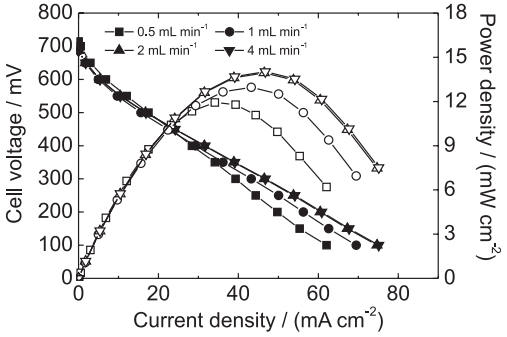

Figure 6. Fuel cell performance for different anode feed flow rates in the alkaline DGFC (glycerol concentration: 1 mol L^{-1}; temperature: 60 °C; KOH concentration: 4 mol L^{-1}; oxygen as comburent with a flow rate of 20 mL min^{-1}).

Mass transfer processes in alkali-based direct alcohol fuel cells can become significant due to the high viscosity of highly loaded KOH solutions compared to neutral ones (only containing alcohol). Furthermore, a large percentage of the products are organic acids that in alkaline medium are in the form of potassium salts, some with limited solubility. The accumulation of these salts within the catalytic and gas diffusion layer and the greater viscosity of the solutions serve to impair mass transfer processes. As a consequence, the flow rate is a key variable for improving the performance of this glycerol based alkaline fuel cell. Illie *et al.*[19] already demonstrated this, reporting an optimum flow rate of approximately 7.5 mL min^{-1} for a 5 cm^2 active electrode area with a Pt loading of 2 mg cm^{-2} prepared from a 40% Pt/C. A direct comparison between both systems is not possible, since the gas diffusion layer they used was different than the one used in this study, the electrode active area was larger and the flow field geometry of the graphite plates was not described. Nevertheless, the results in qualitative terms are in agreement, highlighting the importance of the fuel flow rate.

Preliminary results with binary PtRu/C and Pt_3Sn/C catalysts

Glycerol electroxidation requires oxidized species on the surface of the platinum active sites in order to complete the process, which only takes place at high potential. Less noble metals, such as Ru and Sn, typically used in direct methanol and ethanol fuel cells, respectively, assist in providing oxygenated species at lower potentials.[41] Thus, the binary PtRu/C and Pt_3Sn/C can be interesting candidates for alkaline DGFC. In order to obtain a preliminary assessment of their cell performance, anodes based on these catalysts (commercial materials) were prepared and tested in the cell. Figure 7 displays the corresponding results.

As can be seen, the addition of the second metal had a beneficial effect on cell performance, with an increase in the maximum power density and the OCV. The secondary metal is expected to be a source of oxygenated species that assist in a more rapid oxidation of the glycerol molecule. Looking at the effect of the metal, Sn showed a stronger promotional effect compared to Ru. This behavior may somehow resemble that of ethanol oxidation. The dissociative adsorption of glycerol might be favored due to the greater adsorption strength of the molecule on the platinum sites and the larger Pt-Pt interatomic distance in the Pt_3Sn alloyed phase, which, combined with the donation of oxygenated species from the neighboring Sn ad-atoms, give rise to a more active catalyst. In the case of glycerol electroxidation, adsorption of the molecule on the catalytic surface is a key step due to the presence of three carbon atoms with their corresponding hydroxyl groups.[37] Nevertheless, these latter aspects undoubtedly require

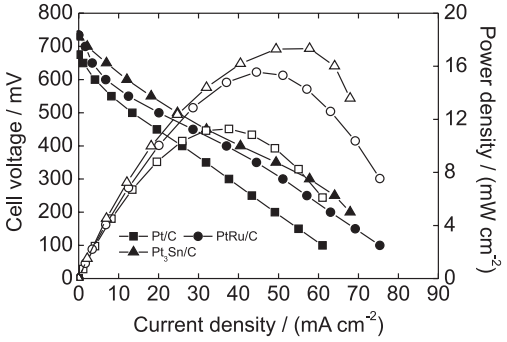

Figure 7. Fuel cell performance with different binary catalysts in the alkaline DGFC (glycerol concentration: 1 mol L^{-1}; temperature: 60 °C; KOH concentration: 4 mol L^{-1}; anode flow rate of 2 mL min^{-1}; oxygen as comburent with a flow rate of 20 mL min^{-1}).

deeper study in order to better understand the role of the secondary metal in the catalyst structure.

One final important comment on this study must be made. If the maximum power densities are compared with those obtained in the literature[21] (Figure 5 of this paper summarizes the state-of-the-art for alkaline DGFC), it can be seen that our values are smaller. However, the experimental conditions used are different from those reported in the literature. On the one hand, the cathode catalyst used in some of the studies reported in the literature was the commercial HYPERMEC™ $FeCuN_4$/C Acta catalyst and a commercial anionic exchange Tokuyama A201 or A901 membrane. Both elements seem to promote cell performance, especially taking into account the small thickness (10 μm) of the commercial membrane and the demonstrated effectiveness of the commercial cathode catalyst, which seems to be very tolerant to alcohol crossover. Furthermore, an anionic exchange ionomer was used in the electrodes (AS-4 anion conductive ionomer, Tokuyama), which helps with OH^- transport within the catalyst layer, increasing the three phase boundary in the electrode necessary to maximize cell performance. Finally, the smaller active area can have a negative impact on cell performance compared to the typical 5 cm^2 used in most studies reported in the literature.[14,19-23]

Nonetheless, the purpose of this paper is to demonstrate the feasibility of implementing a DGFC operating under alkaline conditions with a KOH impregnated PBI membrane, analyze the impact of the operating conditions on the cell performance, and a make final assessment on future ways of improving performance by modifying of the catalyst. Ongoing researches are being carried out in order to produce a better anode catalyst and to develop a specific anionic exchange material based on PBI by modification with anionic exchanger ionic liquids.

Conclusions

This paper has shown the practicality of implementing a direct glycerol fuel cell operating under alkaline conditions with a KOH-impregnated PBI. The operation of this fuel cell showed that a maximum operating temperature of 75 °C is advisable in order to avoid a detrimental increase in the ohmic resistance that offsets the enhancement in the kinetics of the electrochemical reactions. In terms of an adequate glycerol concentration, 1 mol L^{-1} was sufficient to balance fuel availability without massive crossover and limitations imposed on mass transfer processes. Also, the KOH concentration in the fuel plays an important role in promoting cell performance due to its supplying OH^- species necessary for glycerol oxidation. An adequate concentration in order to avoid corrosion problems and mass transfer limitations was 4 mol L^{-1} KOH. The feed flow rate also influenced anode mass transfer processes, with an optimum value of 2 mL min^{-1}, high enough to guarantee a supply of glycerol to the electrode with minimal mass transfer limitations. Finally, PtRu/C and Pt_3Sn/C can be postulated as alternative anode catalysts for enhancing the glycerol electroxidation process, which was reflected in an increase in cell performance compared to the base Pt/C material.

Acknowledgements

The authors want to thank the Electrochemistry Group at Instituto de Química de São Carlos (Universidade de São Paulo) for their generous donation of the gas diffusion layers, the catalysts and the PBI membrane.

References

1. Kiss, A. A.; Ignat, R. M.; *Appl. Energ.* **2012**, *99*, 146.
2. Mota, C. J. A.; da Silva, C. X. A.; Gonçalves, V. L. C.; *Quim. Nova* **2009**, *32*, 639.
3. http://www.anp.gov.br/?dw=8739 accessed in September 2013.
4. http://www.eia.gov/cfapps/ipdbproject/iedindex3.cfm?tid=79&pid=81&aid=1&cid=regions&syid=2007&eyid=2011&unit=TBPD acessed in September 2013.
5. Zhang, Z.; Xin, L.; Li, W.; *Appl. Catal. B-Environ.* **2012**, *119-120*, 40.
6. Carretin, S.; McMorn, P.; Johnston, P.; Griffin, K.; Kiely, C. J.; Hutchings, G. J.; *Phys. Chem. Chem. Phys.* **2003**, *5*, 1329.
7. Bauer, R.; Hekmat, D.; *Biotechnol. Prog.* **2006**, *22*, 278.
8. Jin, C.; Sun, C.; Dong, R.; Chen, Z.; *J. Nanosci. Nanotechnol.* **2012**, *12*, 324.
9. Kwon, Y.; Birdja, Y.; Spanos, I.; Rodriguez, P.; Koper, T. M.; *ACS Catal.* **2012**, *2*, 759.
10. Falase, A.; Garcia, K.; Lau, C.; Atanassov, P.; *Electrochem. Comm.* **2011**, *13*, 1488.
11. Huang, Z.; Li, F.; Chen, B.; Xue, F.; Yuan, Y.; Chen, G.; Yuan, G.; *Green Chem.* **2011**, *13*, 3414.
12. Liang, D.; Gao, J.; Sun, H.; Chen, P.; Hou, Z.; Zheng, X.; *Appl. Catal. B-Environ.* **2011**, *106*, 423.
13. Rodrigues, E. G.; Pereira, M. F. R.; Delgado, J. J.; Chen, X.; Órfão, J. J. M.; *Catal. Comm.* **2011**, *16*, 64.
14. Zhang, Z.; Xin, L.; Li, W.; *Int. J. Hydrogen Energ.* **2012**, *37*, 9393.
15. Simões, M.; Baranton, S.; Coutanceau, C.; *Appl. Catal. B-Environ.* **2011**, *110*, 40.
16. Katryniok, B.; Kimura, H.; Skrzynska, E.; Girardon, J.-S.; Fongarland, P.; Capron, M.; Ducoulombier, R.; Mimura, N.; Paul, S.; Dumeignil, F.; *Green Chem.* **2011**, *13*, 1960.

17. Lee, S.; Kim, H. J.; Choi, S. M.; Seo, M. H.; Kim, W. B.; *Appl. Catal. A-General* **2012**, *429-430*, 39.
18. Matsuoka, K.; Iriyama, Y.; Abe, T.; Matsuoka, M.; Ogumi, Z.; *J. Power Sources* **2005**, *150*, 27.
19. Ilie, A.; Simoes, M.; Baranton, S.; Coutanceau, C.; Martemianov, S.; *J. Power Sources* **2011,** *196*, 4965.
20. Zhang, Z.; Xin, L.; Li, W.; *Appl. Catal. B-Environ.* **2012**, *119-120*, 40.
21. Qi, J.; Xin, L.; Zhang, Z.; Sun, K.; He, H.; Wang, F.; Chadderdon, D.; Qiu, Y.; Liang, C.; Li, W.; *Green Chem.* **2013**, *15*, 1133.
22. Marchionni, A.; Bevilacqua, M.; Bianchini, C.; Chen, Y.-X.; Filippi, J.; Fornasiero, P.; Lavacchi, A.; Miller, H.; Wang, L.; Vizza, F.; *Chem. Sus. Chem.* **2013,** *6*, 518.
23. Zhang, Z.; Xin, L.; Qi, J.; Chadderdon, D. J.; Li, W.; *Appl. Catal. B-Environ.* **2013**, *136-137*, 29.
24. Hou, H.; Sun, G.; He, R.; Wu, Z.; Sun, B.; *J. Power Sources* **2008**, *182*, 95.
25. Hou, H.; Sun, G.; He, R.; Sun, B.; Jin, W.; Liu, H.; Xin, Q.; *Int. J. Hydrogen Energ.* **2008**, *33*, 7172.
26. Hou, H.; Wang, S.; Jiang, Q.; Jin, W.; Jiang, L.; Sun, G.; *J. Power Sources* **2011**, *196*, 3244.
27. Modestov, A. D.; Tarasevich, M. R.; Leykin, A. Y.; Filimonov, V. Y.; *J. Power Sources* **2009**, *188*, 502.
28. Cremers, C.; Niedergesäß, A.; Jung, F.; Müller, D.; Tübke, J.; *ECS Trans.* **2011**, *41*, 1987.
29. Padayachee, D.; Golovko, V.; Marshall, A. T.; *Electrochim. Acta* **2013**, *98*, 208.
30. Zhang, X.; Shen, P. K.; *Int. J. Hydrogen Energ.* **2013**, *38*, 2257.
31. Dector, A.; Cuevas-Muñiz, F. M.; Guerra-Balcázar, M.; Godínez, L. A.; Ledesma-García, J.; Arriaga, L. G.; *Int. J. Hydrogen Energ.* **2013**, *38*, 12617.
32. Yongprapat, S.; Therdthianwong, S.; Therdthianwong, A.; *Electrochim. Acta* **2012**, *83*, 87.
33. Mougenot, M.; Caillard, A.; Simoes, M.; Baranton, S.; Coutanceau, C.; Brault, P.; *Appl. Catal. B-Environ.* **2011**, *107*, 372.
34. Bambagioni, V.; Bianchini, C.; Marchionni, A.; Filippi, J.; Vizza, F.; Teddy, J.; Serp, P.; Zhiani, M.; *J. Power Sources* **2009**, *190*, 241.
35. Simões, M.; Baranton, S.; Coutanceau, C.; *Appl. Catal. B-Environ.* **2011**, *110*, 40.
36. Kwon, Y.; Birdja, Y.; Spanos, I.; Rodriguez, P.; Koper, M. T. M.; *ACS Catal.* **2012**, *2*, 759.
37. Gomes, J. F.; Martins, C. A.; Giz, M. J.; Tremiliosi-Filho, G.; Camara, G. A.; *J. Catal.* **2013**, *301*, 154.
38. Gilliam, R. J.; Graydon, J. W.; Kirk, D. W.; Thorpe, S. J.; *Int. J. Hydrogen Energ.* **2007**, *301*, 359.
39. Balej, J.; *Int. J. Hydrogen Energ.* **1985**, *10*, 233.
40. Zhiani, M.; Gasteiger, H. A.; Piana, M.; Catanorchi, S.; *Int. J. Hydrogen Energ.* **2011**, *36*, 5110.
41. Colmati, F.; Antolini, E.; Gonzalez, E. R.; *J. Power Sources* **2006**, *157*, 98.

Submitted on: October 17, 2013
Published online: January 24, 2014